

Application of New Solutions for Groundwater Mounding to Irrigation Mosaics

Cook, F.J.^{1,2,3}, J.H. Knight^{1,4}, E. Xevi^{3,5}, Z. Paydar^{3,6} and K.L. Bristow^{3,7}

¹CSIRO Land and Water, Indooroopilly, Queensland

²The University of Queensland, St Lucia, Queensland

³Cooperative Research Centre for Irrigation Futures

⁴Griffith University, Nathan, Queensland

⁵CSIRO Land and Water, Griffith, NSW

⁶CSIRO Land and Water, Canberra, ACT

⁷CSIRO Land and Water, Townsville, Queensland

Email: freeman.cook@csiro.au

Keywords: *Irrigation, groundwater, non-dimensional, mosaics*

EXTENDED ABSTRACT

Irrigation mosaics, consisting of patches of irrigated area, may offer advantages when compared to traditional contiguous irrigation schemes (Figure 1). Irrigation mosaics could reduce water table rise, water logging and salinisation associated with large irrigation schemes. The water table mound that builds up under an irrigated patch due to increased recharge is examined using both a new analytical solution and a numerical solution. The rise in water table is examined in both dimensional and non-dimensional parameters with the analytical solution. This solution was developed by Cook et al. (2007a) and is computationally efficient. The use of non-dimensional variables allow us to examine a very large range of possible solutions. A solution for water table rise with a square array of circular irrigation patches is developed and used to examine these arrays. These results are supplemented by numerical simulations using MODFLOW (McDonald & Harbaugh, 1988). The

MODFLOW calculations allow for periodic recharge and also irrigation arrays that are limited in spatial extent.

Results show that the maximum water table rise (in the centre of the irrigated patch) is strongly dependent on the size of the irrigation patch. This water table rise is linear with time initially but the rate of rise reduces with time as the mound spreads. The irrigation arrays show that if mosaics are to be introduced that the size and spacing will have a large effect on the maximum water table rise. The numerical results show that periodic recharge will result in a periodic time rise of the water table and that this is likely to approach the water table rise calculated with an average steady recharge rate over longer time.

Results suggest that irrigation mosaics of correct size and spacing could reduce water table rises relative to traditional irrigation systems while still irrigating the same total area.

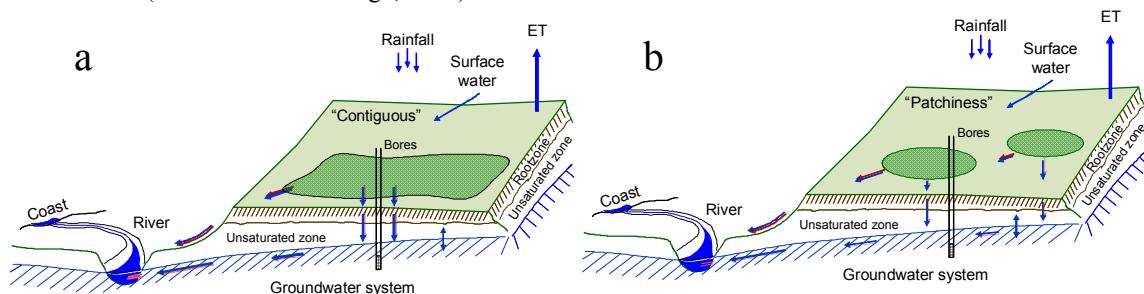


Figure 1. Schematic diagram showing a) traditional contiguous area irrigation and b) irrigation mosaics.

1. INTRODUCTION

Development of irrigation has usually occurred by an *ad hoc* process of individual farmers implementing irrigation at a small scale or by large irrigation schemes. Planned irrigation schemes where the scale of an individual irrigation area is small, but the total area irrigated may be large, are rare. Such schemes we term irrigation mosaics (Paydar et al., 2007a,b; Cook et al., 2007a) and a comparison with a more traditional contiguous area of irrigation is shown in Figure 1.

Although the problems of irrigation as a scale issue have been known for some time “Water-table and salinity problems are to a large degree disabilities of scale; to this degree isolated small or individual irrigation projects are free of them” (England, 1963). There appears to be little published literature on analysing the problem of size in irrigated systems on water table rise, or on spatially distributed systems such as irrigation mosaics on water table rise. Here we will concentrate on the problem of groundwater mounds below circular irrigated areas.

2. THEORY

2.1. Single Isolated Irrigation Patch

The flow of water from a circular irrigated area to the groundwater and the resulting mound this creates (Figure 2) was described by Hantush (1967) and Dagan (1967) using slightly different approaches.

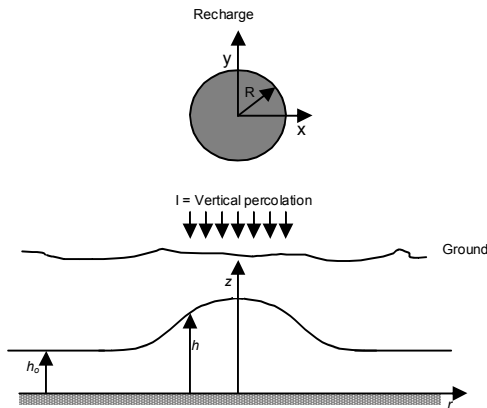


Figure 2. Schematic of flow regime for recharge from a circular irrigated patch to groundwater.

The initial groundwater height is h_0 above an impermeable layer. I is the vertical percolation to the groundwater.

We have followed the approach of Hantush but provided a computationally more efficient solution

which is described in detail by (Cook et al. 2007a). The solution has the following form:

$$H(\rho, \tau) = f(\rho, \tau) = \frac{(h - h_0)\bar{b}K}{R^2 I} \quad (1)$$

where $\rho = r/R$ is the non-dimensional radius, r is the radius [L], R is the radius of the irrigated area [L], $\tau = t\bar{b}K/\phi R^2$ is non-dimensional time, t is time [T], ϕ is the specific yield [$L^3 L^{-3}$], H is the non-dimensional water table height, f is a function defined below, h is the water table height above an impermeable base [L], h_0 is the initial watertable height above an impermeable base [L], I is the recharge rate [$L T^{-1}$], $\bar{b} = (h_m - h_0)/2$ is the linearization parameter [L], $h_m = h(0, \tau)$ is the maximum watertable height at τ and K is the hydraulic conductivity of the aquifer [$L T^{-1}$]. The function f is defined in Cook et al. (2007a) and for $\rho = 0$ and 1 given exactly by:

$$f(0, \tau) = \tau \left[1 - e^{-\left(\frac{1}{4\tau}\right)} \right] + \frac{1}{4} E_1 \left(\frac{1}{4\tau} \right) \quad (2)$$

$$f(1, \tau) = \frac{1}{2} \left[\tau - \int_0^\tau I_0 \left(\frac{1}{2\alpha} \right) e^{\left(\frac{-1}{2\alpha}\right)} d\alpha \right]$$

where E_1 is the exponential integral. Approximate solutions for f are presented by Cook et al. (2007) and are for $\tau < 0.1$:

$$\begin{aligned} \rho < 1 \\ f(\rho, \tau) = \tau \frac{\tau}{\sqrt{\rho}} & \left[\begin{aligned} & \frac{2i^2 \operatorname{erfc} \left(\frac{1-\rho}{2\sqrt{\tau}} \right) + \frac{(3+\rho^{-1})\sqrt{\tau}}{2} i^3 \operatorname{erfc} \left(\frac{1-\rho}{2\sqrt{\tau}} \right)}{16} \\ & - \frac{3(1-\rho^{-1})(5+3\rho^{-1})\tau}{16} i^4 \operatorname{erfc} \left(\frac{1-\rho}{2\sqrt{\tau}} \right) \\ & + \frac{3(35-5\rho^{-1}+9\rho^{-2}+25\rho^{-3})\tau^{3/2}}{64} i^5 \operatorname{erfc} \left(\frac{1-\rho}{2\sqrt{\tau}} \right) \\ & - \frac{15(1-\rho^{-1})(315+287\rho^{-1}+305\rho^{-2}+245\rho^{-3})\tau^2}{1024} i^6 \operatorname{erfc} \left(\frac{1-\rho}{2\sqrt{\tau}} \right) \end{aligned} \right] \\ \rho > 1 \\ f(\rho, \tau) = \frac{\tau}{\sqrt{\rho}} & \left[\begin{aligned} & \frac{2i^2 \operatorname{erfc} \left(\frac{\rho-1}{2\sqrt{\tau}} \right) - \frac{(3+\rho^{-1})\sqrt{\tau}}{2} i^3 \operatorname{erfc} \left(\frac{\rho-1}{2\sqrt{\tau}} \right)}{16} \\ & - \frac{3(1-\rho^{-1})(5+3\rho^{-1})\tau}{16} i^4 \operatorname{erfc} \left(\frac{\rho-1}{2\sqrt{\tau}} \right) \\ & - \frac{3(35-5\rho^{-1}+9\rho^{-2}+25\rho^{-3})\tau^{3/2}}{64} i^5 \operatorname{erfc} \left(\frac{\rho-1}{2\sqrt{\tau}} \right) \\ & - \frac{15(1-\rho^{-1})(315+287\rho^{-1}+305\rho^{-2}+245\rho^{-3})\tau^2}{1024} i^6 \operatorname{erfc} \left(\frac{\rho-1}{2\sqrt{\tau}} \right) \end{aligned} \right] \quad (3) \end{aligned}$$

and for $\tau \geq 0.1$:

$$f(\rho, \tau) = \tau \left[1 - \exp \left(\frac{-1}{4\tau} \right) \right] + \frac{1}{4} E_1 \left(\frac{1}{4\tau} \right) - e^{\left(\frac{-1}{4\tau}\right)} \left(\frac{\rho^2}{4} + \frac{\rho^4}{256\tau^2} \right), \rho < 1 \quad (4)$$

$$f(\rho, \tau) = \frac{1}{4} E_1 \left(\frac{1}{4\tau} \right) + e^{\left(\frac{-\rho^2}{4\tau}\right)} \left(\frac{1}{32\tau} - \frac{1}{768\tau^2} + \frac{\rho^2}{3072\tau^3} \right), \rho > 1$$

The $i^n \text{erfc}(x)$ functions are the repeated integrals of the error function and are calculated by (Carslaw and Jaeger 1959, p483):

$$\begin{aligned} i^0 \text{erfc}(x) &= \text{erfc}(x) = 1 - \text{erf}(x) \\ i \text{erfc} &= \frac{1}{\sqrt{\pi}} \exp(-x^2) - x \cdot \text{erfc}(x) \\ 2n i^n \text{erfc}(x) &= i^{n-2} \text{erfc}(x) - 2x \cdot i^{n-1} \text{erfc}(x) \\ n &= 2, 3, \dots \end{aligned} \quad (5)$$

where $\text{erfc}(x)$ is the complementary error function.

The non-dimensional results can be converted to dimensional values by calculating:

$$\begin{aligned} h_m &= \sqrt{\frac{2H_m R^2 I}{K} + h_0^2} \\ \bar{b} &= (h_m + h_0) / 2 \end{aligned} \quad (6)$$

where $H_m = f(0, \tau)$ and then using eqn (3) or (4) to obtain H for other values of ρ and values of $h(r, t)$ from eqn (1) and r and t from their definitions.

2.2. Mosaic Arrays - Analytical

We will assume that an infinite array of circular irrigation patches with the same radius are arranged in a square grid with spacing (in the non-dimensional space) between the centre of the patches of $L \geq 2$ (i.e. in physical terms $L > 2R$) (Figure 3) and L is an integer. Calculations only need to be made along an axis because of radial symmetry.

The water table height can then be determined in the space around a patch for $0 \leq \rho \leq L/2$ using the principle of superpositioning and results in:

$$\begin{aligned} H_n(\rho, \tau) &= H_{n-1}(\rho, \tau) + H((nL - \rho), \tau) + H((nL + \rho), \tau) \\ &+ 2 \sum_{i=1}^n \left[\begin{aligned} &H\left(\sqrt{(nL - \rho)^2 + (iL)^2}, \tau\right) + H\left(\sqrt{(nL + \rho)^2 + (iL)^2}, \tau\right) \\ &+ H\left(\sqrt{(nL)^2 + ((n-i)L - \rho)^2}, \tau\right) \\ &+ H\left(\sqrt{(nL)^2 + ((n-i)L + \rho)^2}, \tau\right) \end{aligned} \right] \\ &- H\left(\sqrt{(nL)^2 + \rho^2}, \tau\right) \\ H_0(\rho, \tau) &= H(\rho, \tau) \\ n &\in I \end{aligned} \quad (7)$$

The value of n is obtained from the fact that H tends towards zero as ρ increase. We choose a value of ρ_n which is an integer such that $H(\rho_n) \approx 10^{-6} H_m$ and then $n = \text{int}(\rho_n / L) + 1$.

Equation (7) allows us to explore the effect of τ , ρ and L on H . Although the H is inversely proportional to R^2 which means that for large R only small values of H result but in dimensional

terms change in watertable height ($h - h_0$) is large due to the proportional relationship to R^2 indicated by eqn (1).

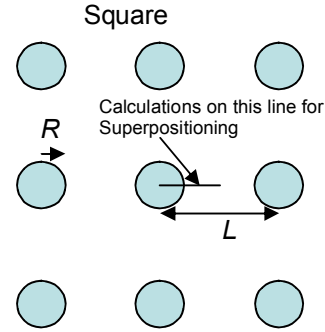


Figure 3. Schematic of square grid for mosaic calculations.

Programs were written in MatLab to solve eqns (2) to eqn (6). This is a good programming environment as routines are available to solve $E_1(\text{xpint}(x))$ and $\text{erfc}(x)$. The results were directly ported to EXCEL spreadsheets using the *xlswrite* command and any further manipulation to dimensional values done within the spreadsheets. Testing of the programs was done using the original equations of Hantush and they were found to give exactly the same results. The results were also checked against the MODFLOW results for the single patch for the first stress period and found to give similar results.

2.3. Mosaic Arrays - Numerical

Numerical solutions using MODFLOW (McDonald & Harbaugh 1988, Harbaugh et al. 2000) were carried out for a single patch and square grid (Figure 4). The area irrigated is the same in both irrigation patterns. The flow domain is 120 X 120 km with one layer 20 m thick and bounded on all sides by a free flow boundary condition. The aquifer is unconfined and with properties; $K = 160 \text{ m day}^{-1}$, $\phi = 0.06 \text{ m}^3 \text{ m}^{-3}$, $h_0 = 5 \text{ m}$ and $I = 0.002 \text{ m day}^{-1}$.

The aquifer is recharged for 120 days at a rate of I and then zero recharge for 240 days. This cycle is repeated 3 times resulting in 6 stress periods.

The pre- and post- processors available in processing MODFLOW (PMWIN) were used to prepare data input and perform ground water numerical simulation on patches of different sizes and configurations.

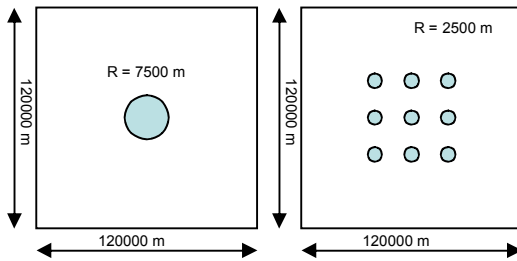


Figure 4. Schematic of domain and irrigation patches for single and square array in MODFLOW.

3. RESULTS

3.1. Water Table Rise from a Single Patch

Over short time periods the water table shape is similar to a square wave, as the system does not ‘know’ about the outer boundary (Figure 5a). Over longer time periods the water table shape becomes more curvilinear (Figure 5).

Also over short times the value of H_m and value of H for $\rho < 0.9$ is approximately equal to τ (Figure 5a, b). With increasing time the mound gets large in terms of its height and the extent it spreads into the area surrounding the patch.

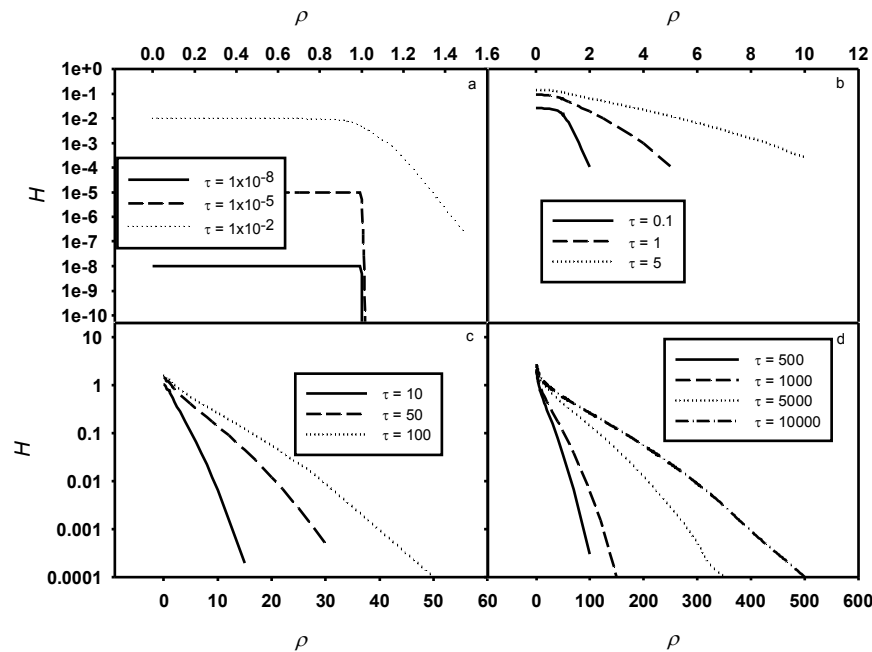


Figure 5. H versus ρ for various values of τ . Note the scales for ρ are different for each panel.

The effect of water table rise at the centre of the patch in dimensional variables shows that initially the water table rises linearly with time (Figure 6). This linear rise decreases with time to a logarithmic rate of rise as can be seen in Figure 6. The time of when this logarithmic rate of rise becomes noticeable increases as R increases and for $R = 100$ km the water table is still rising approximately linearly after 100 years.

The numerical simulation gives results which show the effect of the periodicity in the recharge function (Figure 7). The numerical and analytical results are almost identical for the centre point during the first stress period.

The average flux values show that by the end of the sixth stress period the periodic solution is tending towards the solution for the mean flux. This is especially so at greater distance from the centre where the fluctuations are damped.

The numerical solution also predicts a rise in the water table at $r = 8000$ and 9500 m sooner than the analytical solution does (data not shown). This is likely due to numerical dispersion within the numerical simulations.

3.2. Water Table Rise for an Array of Patches

For the analytical solutions the spacing at which the array approaches an isolated patch and the

maximum water table height increases as τ increases (Figure 8) except for $\tau = 0.1$ (Figure 8a). At large time and small array spacing the water table is essentially flat and for $L = 2$ is similar to that of a planar recharge source (Figure 8c, d).

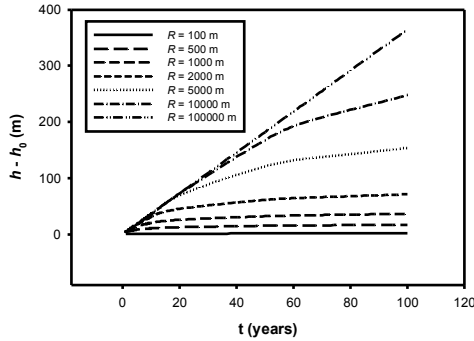


Figure 6. Change in maximum water table height ($h_m - h_0$) versus time (t) for various values of R . The parameters used were; $K = 1 \text{ m day}^{-1}$, $I = 1 \times 10^{-3} \text{ m day}^{-1}$, $\phi = 0.1 \text{ m}^3 \text{ m}^{-3}$ and $h_0 = 10 \text{ m}$.

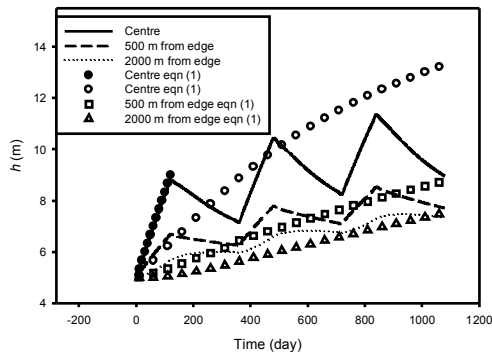


Figure 7. Water table rise versus time under a single patch with $R = 7500 \text{ m}$. The lines shown are for the centre (h_m), $r = 8000 \text{ m}$ and $r = 9500 \text{ m}$. The solid circles are calculated with eqn (1) using the maximum recharge rate ($I = 0.002 \text{ m day}^{-1}$) for the centre. The open symbols are calculated with eqn (1) with the mean recharge rate ($I = 0.00067 \text{ m day}^{-1}$)

The spacing at which the water table height approaches that of an isolated patch increases with τ . Although we consider $\tau = 0.1$ to be a small time for the system the physical time can be quite large when R is large, for example for $R = 100 \text{ km}$, t is 27,384 years when $\tau = 0.1$, while for $R = 100 \text{ m}$, t is 10 days for the same value of τ .

The maximum water table height for the array of patches increases compared to an isolated patch, as L decreases and τ increases (Figure 9). This means that as R increases, τ increases and the spacing

between patches to minimise water table rise would have to increase. The numerical simulations show similar results but with the periodicity of the recharge now included. Taking the time when recharge occurs as continuous the results shown in Figure 10 for water table contours correspond to $\tau = 0.77$ ($t = 120$), $\tau = 1.55$ ($t = 240$ day of continuous recharge) and $\tau = 2.32$ ($t = 360$ day of continuous recharge). The spacing between the patches is 17.5 km which results in $L = 7$. For the first 2 stress periods the array in the numerical simulation gives results the values of n are approximately 3 and 5, which are comparable with results from the analytical solutions for $\tau = 0.1$ and 1 respectively. The result for the first stress period are similar to that predicted with the analytical method with isolated patch occurring (Figure 8a, 10a). Similarly for the second stress period we see that the water tables are just starting to interact, this is what would be predicted from the analytical method.

By stress period 6 (Figure 10c) there is a large amount of interaction between the patches and this cannot be compared with the analytical solution as the finite nature of the numerical model now has an effect on the results.

The increase in water table heights is not as high for mosaics as the single patch (Figure 6, 7). The rise in water table is more curved in figure 11, which is mainly due to the radius being smaller. This same curvature in water table rise is predicted using the analytical model with the average recharge rate (figure 11).

The analytical results shown in Figure 11 are for a single patch as there is very little overlap in water tables that will occur during the time shown. Again the numerical periodic solutions are tending towards the average constant rate analytical solution as time increases. This result suggests that large water table rises will occur with large irrigation areas and is entirely inherent to the size of the system.

4. DISCUSSION

Here we have quantified England's (1963) statement on the size of irrigated area with regard to the effect on water tables, and have shown that water table rise is strongly dependent on the radius of the irrigated area (Figure 6). These results also show that initially water table rise is approximately linear with time. This result suggests that large water table rises will occur with large irrigation areas and is entirely determined by the size of the system.

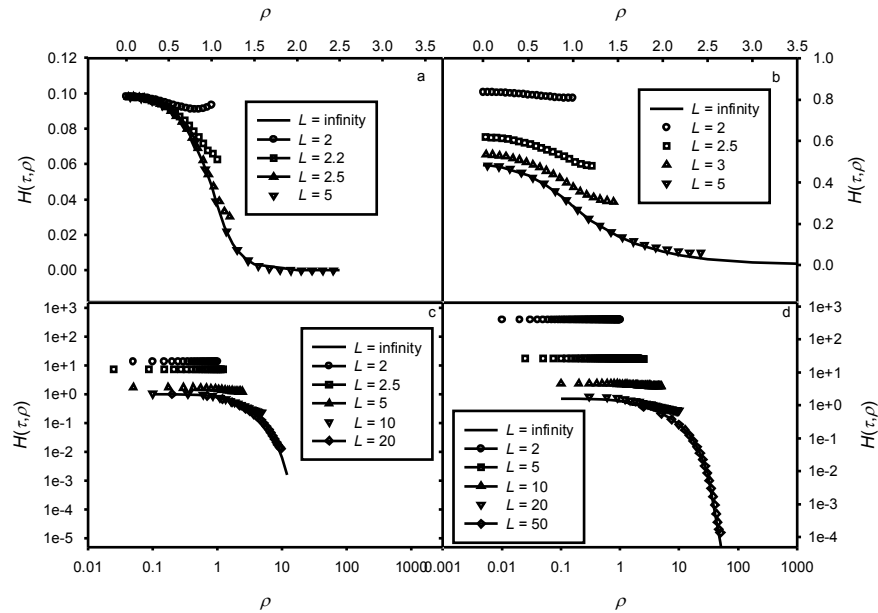


Figure 8. H versus ρ for a square array of circular irrigation patches at a) $\tau = 0.1$, b) $\tau = 1$, c) $\tau = 10$ and d) $\tau = 100$.

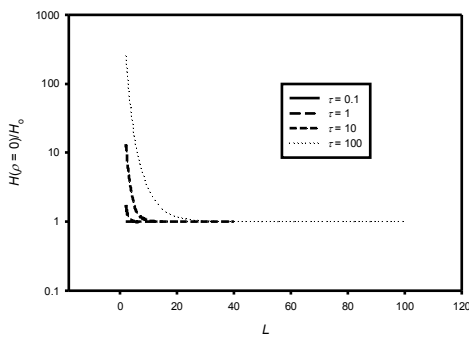


Figure 9. The maximum water height in the centre of an irrigated patch in an array of patches ($H(\rho = 0)$) compared to an single isolated patch (H_0) versus L , for various values of τ .

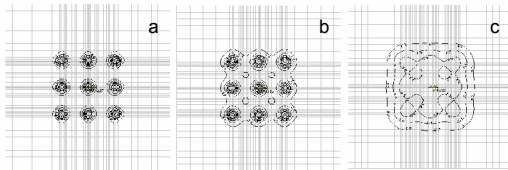


Figure 10. Water table contours for the square array of irrigation patches at a) $t = 120$ day (end of stress period 1), b) 480 day (end of stress period 3) and c) end of stress period 6).

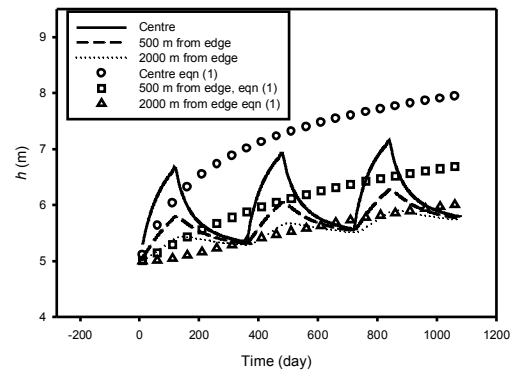


Figure 11. Water table height versus time of the array with 9 patches with $R = 2500$ m. The lines shown are for the centre (h_m), $r = 8000$ m and $r = 9500$ m. The open symbols are calculated with eqn (1) with the mean recharge rate ($I = 0.00067$ m day $^{-1}$) from a single patch.

Given that to prevent salinisation of the root zone leaching is required (Cook et al. 2007b) water table rise of significant proportions is inevitable. This does not seem to have been discussed before even though it is inherent in the Hantush (1967) solutions. Dagan (1967) found that a sloping impermeable base resulted in a displacement down slope of the peak in the water table at small times but at large times slope had almost not effect on the position or height of the water tables. The only physical process that could change the time course for the water tables are if water leaks through the

impermeable base or there is a sink (river, leakage to ocean or well) that the water can flow to. Even with such sinks the resulting water table rise may still be significant (Rassam et al. 2005). It is possible to extend the analysis presented here for combinations of sources and sinks and we hope to be able to do this in the future.

Extending this to irrigation mosaics we can see that the spacing and size of the irrigation patches will determine the water table rise with time along with the aquifer properties and recharge rate. The analytical analysis presented offers a method for rapid investigation of possible sizes and spacing. However, this does not allow for variability in the aquifer properties in space or recharge rate in time. We are working on solving the latter problem and an analytical solution is possible. To deal with spatial variability in aquifer properties will require numerical methods.

The analysis here can be used to assess the marginal impact of irrigation mosaics and size of patches. This is examined in detail by Cook *et al.* (2007a). Irrigation mosaics if they have correct size and spacing could reduce water table rises while irrigation of the same total area occurs (Figures 6, 9).

5. CONCLUSION

Analytical and numerical solutions are used to assess water table mounds created by irrigation. These results are consistent with each other and show that the water table rise is strongly dependent on the size of the irrigated area.

Irrigation mosaics are investigated and found to reduce water table rise depending on the irrigation patch size and spacing of the patches.

6. ACKNOWLEDGMENTS

This work formed part of a suite of activities carried out through the Northern Australia Irrigation Futures (NAIF) project. It was funded in part by CSIRO, the Land and Water Australia National Program for Sustainable Irrigation (NPSI), the CRC for Irrigation Futures, and the Australian, Western Australia, Northern Territory, and Queensland Governments.

7. REFERENCES

Carslaw H.S. and J.C. Jaeger (1959), *Conduction of Heat in Solids* 2nd edition, Oxford University Press, London, 510p.

Cook F.J., E. Xevi, J.H. Knight, Z. Paydar and K.L. Bristow (2007a), Analysis of biophysical processes with regard to advantages and disadvantages of irrigation mosaics, *CSIRO Land and Water Technical Report*, (In press) 65p.

Cook F.J., N.S. Jayawardane, D.W. Rassam, E.W. Christen, J.W. Hornbuckle, R.J. Stirzaker, K.L. Bristow and T. K. Biswas (2007b), The state of measuring, diagnosing, ameliorating and managing solute effects in irrigated systems, *Cooperative Research Centre for Irrigation Futures Technical Report*, 04/06, 47p.

Dagan G. (1967), Linearized solutions of free-surface groundwater flow with uniform recharge, *Journal of Geophysical Research* 72, 1183-1193.

England, H.N. (1963), Problems of irrigated areas, *In Water Resources and Land Use*, Melbourne University Press, 399-418.

Hantush M.S. (1967), Growth and decay of groundwater-mounds in response to uniform percolation, *Water Resources Research*, 3, 227-234.

Harbaugh A.W., E.R. Banta, M.C. Hill and M.G. McDonald (2000), MODFLOW-2000, The U.S. Geological Survey modular groundwater model User guide to modularization concepts and the ground-water flow process, U. S. Geological Survey, Open-file report 00-92.

McDonald, M.C. and W. Harbaugh (1988), MODFLOW, A modular three-dimensional finite difference groundwater flow model, Open-file report 83-875, Chapter A1, US Geological Survey, Washington DC.

Paydar Z., F.J. Cook, E. Xevi and K.L. Bristow, (2007a), Review of the current understanding of irrigation mosaics, *CSIRO Land and Water, Technical Report* (In press).

Paydar, Z., F.J. Cook, E. Xevi, and K.L. Bristow (2007b), Irrigation Mosaics. How are they different? MODSIM07.

Rassam D.W., G. Walker, and J.H. Knight (2005), Application of the unit response equation to assess salinity impacts of irrigation development in the Mallee, *CSIRO Technical Report* 23p.